Nuclear Instruments and Methods in Physics Research A 602 (2009) 477–483

Contents lists available at ScienceDirect

Nuclear Instruments and Methods in Physics Research A

journal homepage: www.elsevier.com/locate/nima

A rotating modulation imager for locating mid-range point sources

B.R. Kowash [a,*,1], D.K. Wehe [a], J.A. Fessler [b]

[a] Department of Nuclear Engineering and Radiological Science, University of Michigan, Ann Arbor, MI 48109, USA
[b] Department of Electrical Engineering and Computer Science, University of Michigan, Ann Arbor, MI 48109, USA

ARTICLE INFO

Article history:
Received 10 July 2008
Received in revised form
4 December 2008
Accepted 24 December 2008
Available online 19 January 2009

Keywords:
Rotating modulation collimators
Mechanical collimation
Gamma ray imaging
Homeland security

ABSTRACT

Rotating modulation collimators (RMC) are relatively simple indirect imaging devices that have proven useful in gamma ray astronomy (far field) and have more recently been studied for medical imaging (very near field). At the University of Michigan a RMC has been built to study the performance for homeland security applications. This research highlights the imaging performance of this system and focuses on three distinct regions in the RMC field of view that can impact the search for hidden sources. These regions are a blind zone around the axis of rotation, a two mask image zone that extends from the blind zone to the edge of the field of view, and a single mask image zone that occurs when sources fall outside the field of view of both masks. By considering the extent and impact of these zones, the size of the two mask region can be optimized for the best system performance.

Published by Elsevier B.V.

1. Introduction

The time modulation of radiation source distributions has been studied for both astronomical and medical physics applications, but has seen little application in the field of homeland security [1–7]. One class of time modulated systems is the rotating modulation collimator (RMC). One of the most appealing characteristics of this particular design is that they do not require position sensitive detectors in order to locate sources of interest. This feature allows for a significant amount of flexibility in not only detector material selection, but also in the geometry and size of the detectors employed. It also offers a simple way to enhance the current DHS network of non-position sensitive detectors by offering a point source imaging system that snaps on to the front of detectors like the ORTEC DETECTIVE. The focus of this paper is on a RMC system that has been developed for locating hidden point sources in a mid-range (1–50 m) field.

2. Background

In the case of a RMC system, a set of two or more attenuating masks are separated by a known distance as shown in Fig. 1a. One typical pattern for the masks is straight parallel slits made of tungsten or lead for gamma ray imaging. When the masks are rotated together, the photons counted by the detector from any source that is off of the centerline axis will be modulated as the slits appear to the source to open and close producing the pattern shown in Fig. 1b. Both the frequency of the peaks as well as the phase of the pronounced dip contains the information necessary to locate the source by applying an appropriate reconstruction algorithm.

In the field of astronomy, several methods have been developed to compute the transmission function for a given RMC configuration [1–3]. These methods generally assume that the source is located in the far field region so that the RMC sees the incoming photons as parallel rays. For simplicity, the following assumptions are often used: the masks have no thickness, the masks are perfectly opaque, and the detector has infinite extent. More recent research by Sharma et al. [7] has investigated the performance of RMC in the very near field for medical imaging applications.

One of the motivating factors for using RMCs is their ability to achieve excellent angular position resolution (Θ) over a relatively wide field of view (FOV). The angular resolution is a measure of the distance over which two independent sources can be completely resolved and is given by

$$\Theta = \frac{\frac{1}{2}p}{L}, \tag{1}$$

where p is the pitch between slits and L is the separation distance between the two masks.

The FOV defines a source region over which the RMC can be used to accurately detect sources. Once a source moves beyond the FOV of the two mask system there is no longer enough information to produce an accurate image. The FOV for the RMC is

* Corresponding author. Tel.: +1 937 255 3636x4571.
E-mail address: benjamin.kowash@afit.edu (B.R. Kowash).

[1] The views expressed in this article are those of the author and do not reflect the official policy or position of the United States Air Force, Department of Defense, or the U.S. Government.

0168-9002/$ - see front matter Published by Elsevier B.V.
doi:10.1016/j.nima.2008.12.233

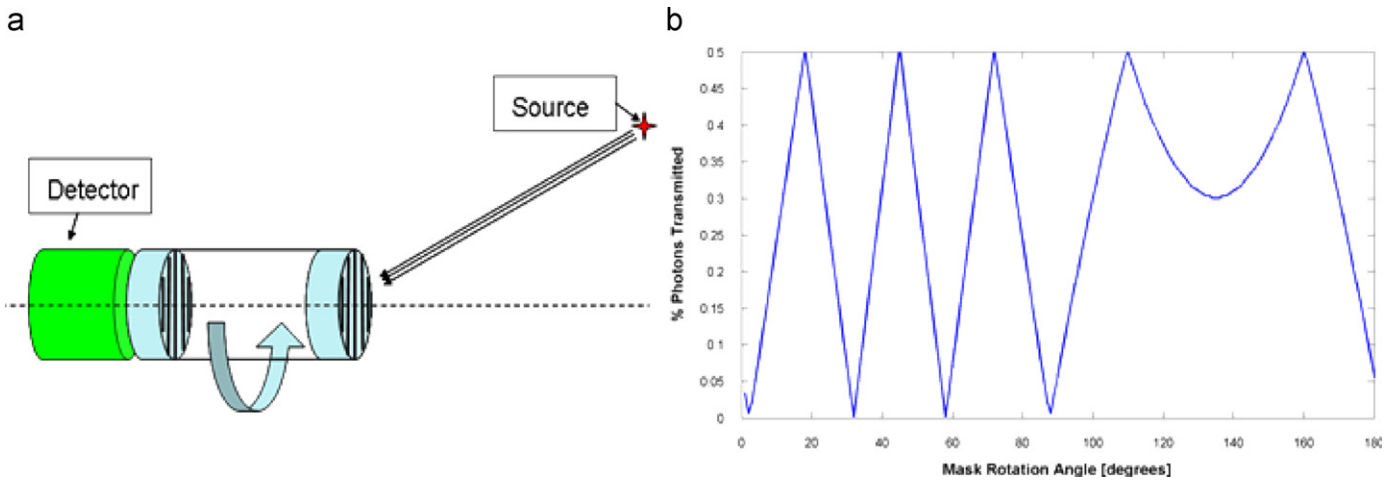

Fig. 1. (a) One possible configuration of a RMC system. As the mask pair is rotated together, the slit pairs will appear to move across each other for any source located off the centerline axis. This has the effect of either blocking the source or allowing photons to pass to the detector. This produces the characteristic modulated detector response for a far field source as seen simulated in (b).

defined as

$$\mathrm{FOV}_{\mathrm{RMC}} = \frac{d}{L} \tag{2}$$

where again L is the separation distance between masks and d is the mask diameter. Typically the pitch between slits and mask diameter are fixed parameters that are defined at the time the mask is cut. The mask separation however, can easily become a free parameter by designing the system so that the front mask can slide back and forth along the axis of rotation. The user can therefore enhance the angular resolution by extending the front mask, at a cost of a reduced FOV. Similarly, collapsing the front mask will increase the FOV at a cost of decreased angular resolution.

3. RMC system design

The RMC system design for this research is fairly simple. The system, as shown in Fig. 2 consists of an outer support tube that is set into a mount. Two large bore bearings (5 in. OD, 4 in. ID) are pressed into this tube, and are used to support a second "driver" tube. A timing belt pulley is mounted onto the midsection of this driver tube which couples to a stepper motor coupled to an Applied Motion Si3540. A Renishaw encoder ring is also mounted on the driver tube, and is used to provide the angular position of the RMC system, with 1.2 arc minutes of resolution. The encoder ring is read out by a Renishaw RGH20 optical read head, which is attached to the support tube. The driver tube is inserted into the support tube through the bearings, and fixed into place, allowing it to freely rotate, but not slide back and forth.

A third "flight" tube containing the RMC masks is then inserted into the driver tube. The first mask is set into the detector end of the flight tube and locked into place. A second mask is secured in an aluminum carrier that is inserted into the other end of the flight tube. This aluminum carrier can freely slide back and forth down the length of the tube until locked in place, and allows for the distance between masks to become a free parameter when imaging (up to 50 cm for this system).

The RMC masks for this study were not optimized, but rather were selected to ensure functionality. The slits and slats are relatively large, as is the thickness of the material. Two identical masks were cut out of a 12.7 mm thick piece of lead using wire electrical discharge machining (EDM). The slits and slats are equal width of 4 mm and a pitch of 8 mm. The diameter of the masks is

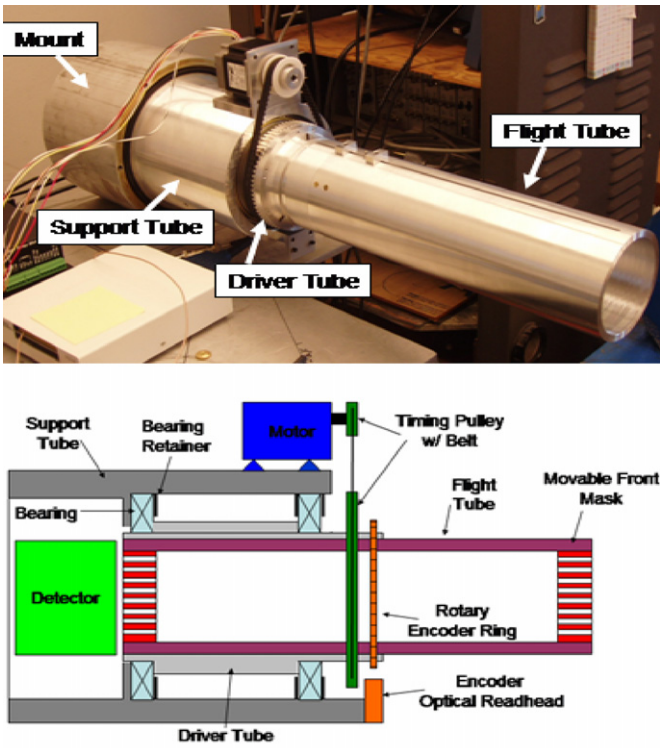

Fig. 2. Illustration of the RMC system design.

38.1 mm for a total of 8 slits and 8 slats per mask. It should be noted that the design of this RMC allows any number of mask patterns, as well as multiple numbers of masks. Using Eqs. (1) and (2) and the design parameters, the maximum resolution for the RMC is ~0.5° with a ~9° FOV.

4. RMC operation and data processing

Another benefit of RMCs is the relative simplicity of the data acquisition systems needed to generate point source images. As the RMC is rotated, the angular position of the system provided by the encoder–decoder system is recorded along with the total number of counts under the photopeak of interest using a 3 × 3 in.

sodium iodide detector. The angular position data is then combined with the counting data in Labview to produce the RMC transmission function seen in Fig. 3a.

For this research a maximum likelihood-expectation maximization (ML-EM) algorithm similar to the one described by Shepp and Vardi is used to reconstruct the final image [9]. The iterative ML-EM method takes the form

$$\lambda_j^{n+1} = \frac{\lambda_j^n}{\sum_i a_{ij}} \sum_i a_{ij} \left(\frac{y_i}{\sum_k \lambda_k^n a_{ik} + b_i} \right) \quad (3)$$

where λ is a vector containing the image estimate, a_{ij} is a system matrix that contains the probabilities that a photon emitted from the jth source pixel is detected in the ith RMC mask position, y is a vector containing the measured RMC data, and b is the unmodulated background. Reconstructing an image using the ML-EM method requires knowledge of the transmission probabilities (Fig. 1b) from a field of potential source locations to the detector via the mask system. These probabilities, which form the matrix a_{ij} are computed by dividing the source plane at a known distance into a vector of pixels. Each column of the system matrix a_{ij} contains the simulated RMC transmission function that would be measured if the source were located in the jth pixel.

In order to simulate the RMC transmission functions (and hence develop the matrix a_{ij}), an appropriate model of the system is required as a function of the source position. Because homeland security applications range from the near to mid-field the far field models traditionally used are not applicable. As a result a new system model was developed that accounts for all of the RMC system design parameters such as mask thickness, material, pattern design, separation, and measurement time per RMC position. The new model takes advantage of the fact that the photons from the source essentially project an image of the front mask onto the rear mask. By computing the location of the projected front mask with respect to the rear mask and detector, it is possible to directly compute the fraction of the detector area that is exposed to the source. As the masks rotate the projection of the front mask will shift and at some points the slits will be closed and at other points open, producing the characteristic RMC transmission functions. The details of this process will be presented in a separate paper, where predictions using the model will be shown to match very well with data taken using the prototype RMC. This new system model was used to generate images like the one shown in Fig. 4b for this research. Because the RMC masks are symmetric, the transmission function is completely mapped with every half rotation of the system. As previously reported, this produces a 180° ambiguity in the reconstruction, which can be resolved by making two measurements with different RMC positions [1–3].

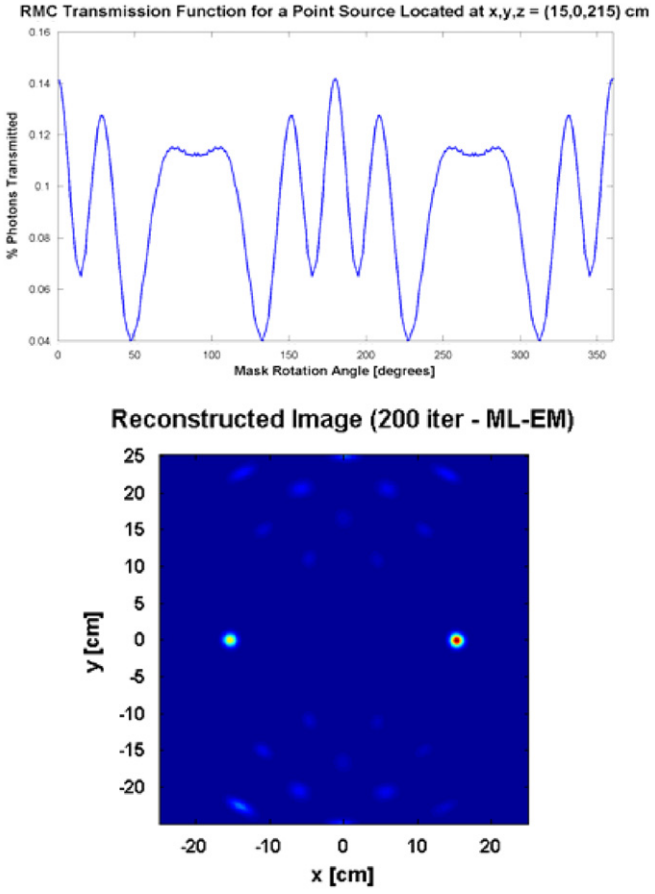

Fig. 3. This is the RMC transmission function and ML-EM reconstructed image (200 iterations) measured using the prototype RMC, for a Ba-133 point source at $x,y,z = (15,0,215)$ cm. The 180° ambiguity seen here occurs because the masks are symmetric over 180° of rotation. Also note that the transmission function shown in the top panel has a maximum of ~0.14 and a minimum of ~0.4. This compression (vice max = 0.5, min = 0) is a result of the source being located in the near field. In the near field the projection of the front mask onto the rear mask is magnified resulting in a non-uniform overlap of the slits and slats.

The 180° ambiguity can also be removed by changing the design parameters of the masks so that the system is no longer symmetric. Fig. 4 shows simulation results of the RMC transmission function and reconstructed image when the masks are symmetric (left panels) and asymmetric (right panels) for a point source located 1000 cm from the RMC. In the symmetric case the masks are the same those described in the RMC system design. In asymmetric case the grid pattern in the front mask is shifted 2 mm off axis, so that the mask pattern is not symmetric about the RMC centerline, causing the two masks to be out of phase with each other. The cost for making the masks asymmetric is a reduction in modulation efficiency (defined as the ratio of the lowest to highest peak) by $<1\%$ and a reduction in the geometry efficiency (fraction of photons incident on the top of the RMC that hit the detector) by $<3.6\%$.

5. Mapping the RMC and position error estimation

Because the source location and intensity are typically unknown, it is important to understand how the reconstructed position estimate behaves as the source is moved around the FOV. Two-dimensional mapping of the system was accomplished using a Ba-133 source located 215 cm from the front mask of the detector. The distance between the masks was fixed at $L = 24$ cm. The source was placed on a two axis Velmex bi-slide stepper motor system that allows the source to translate in both the x- and y-dimensions with sub-millimeter accuracy. The system response was then mapped by taking measurements within the right lower quadrant of the system FOV. Due to the symmetric nature of the system, the mapping of a single quadrant is sufficient to determine the system response in the other quadrants.

For each map location the position error is obtained using a bootstrap procedure that has been described elsewhere [8]. The bootstrap method for the RMC studied is very straightforward. Suppose that for a known measurement time, the RMC rotates N times. For each complete rotation, a length P vector is created, where P is the number of discrete RMC rotation bins where data is recorded (i.e. $\omega t = 1,2,\ldots,360°$, $\omega \equiv$angular velocity of RMC, $t \equiv$sample time). Each of these vectors will be independent identically distributed (IID) with respect to each other. The measured RMC transmission function is simply the sum of these N vectors in the order they are recorded. The bootstrap procedure

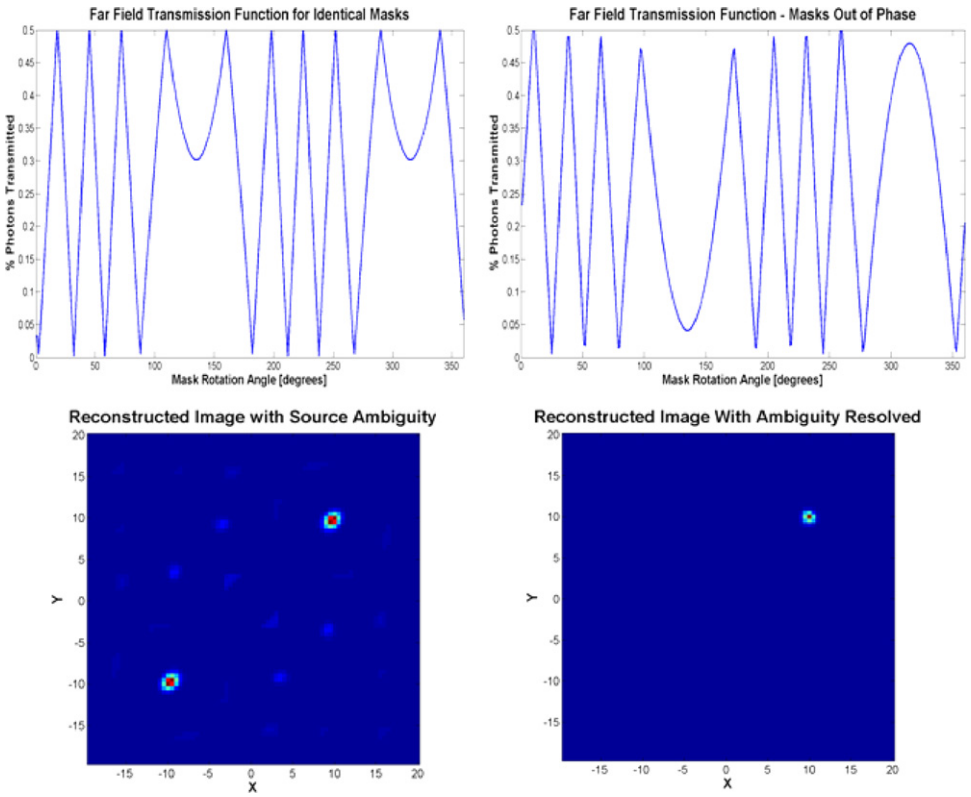

Fig. 4. A RMC simulation with a far field source highlights the 180° ambiguity that results from symmetric masks (left panel). When the masks are made asymmetric (right panels) the ambiguity can be resolved with a single measurement. The cost of making the masks asymmetric is a reduction in the RMC modulation and geometric efficiency.

Table 1
This shows how the data is recorded as the RMC rotates. The final modulation function is simply the sum of all the counts each discrete rotation angle ωt. For a bootstrap technique, a new modulation function T_{new} is created by random resampling of the columns N times and summing the results.

	R_1	R_2	…	R_N	T_{data}
ωt_1	$R_1(\omega t_1)$	$R_2(\omega t_1)$	…	$R_N(\omega t_1)$	$\sum$ row 1
ωt_2	$R_1(\omega t_2)$	$R_2(\omega t_2)$	…	$R_N(\omega t_2)$	$\sum$ row 2
…	…	…	…	…	
ωt_P	$R_1(\omega t_P)$	$R_2(\omega t_P)$	…	$R_N(\omega t_P)$	$\sum$ row P

resamples with replacement, N of the complete set of vectors and the sum of these resampled vectors produces a new transmission function that is slightly different than the original measured function. An image is generated for the original data as well as for each set of resampled data and the position estimate of the source is recorded for each image. This procedure is repeated hundreds of times and the standard deviation in the position estimate can be calculated. This process is shown in Table 1.

6. Results of RMC measurements

The RMC mapping for this research covers three distinct regions. The first region is a blind zone that starts at the center of the RMC FOV and has an extent equal to the resolution of the RMC given in Eq. (1). When the source is located at $\rho = 0$ (i.e. RMC centerline) the RMC transmission function is flat because the masks remain stationary as viewed by the source. Because of this flat pattern is it impossible to distinguish a source located on the central axis from background when using a single RMC. As the source moves off axis, the transmission pattern (Fig. 1b) begins to develop but is not fully developed until it is past a certain threshold given by the RMC resolution (Eq. (1)). Due to weak modulation and statistical noise on the data, the location of sources in this region can be difficult if not impossible to estimate.

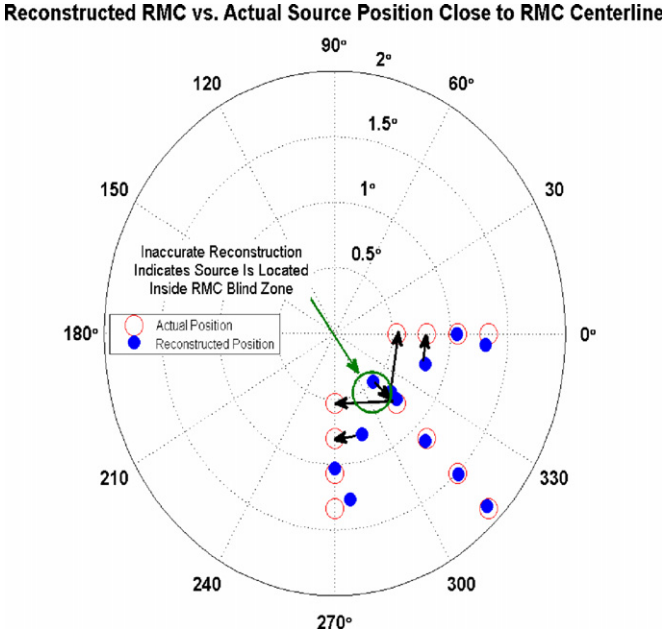

Fig. 5. The RMC blind spot measured using the prototype RMC is illustrated here as the region from $\rho = 0$ to ~0.7°, where the modulation pattern is too uniform to allow for accurate reconstructions. The system resolution, which defines the width of the blind zone is 0.955° and matches well with the measured data.

Fig. 5 shows the results of mapping data points every cm in x-, y- and x–y. From the data it is seen that the RMC blind spot ($L = 24$ cm) extends to ~0.7°. Additionally, the region from 0.7° to ~1.0° could be said to be fuzzy, since the position estimate is still not accurate, but is clearly approaching the true position. The system resolution for the system ($p = 8$ mm, $L = 24$ cm) is 0.955°, which matches very well with the measurements.

Because the width of the blind zone is defined by the system resolution, the simplest way to minimize its extent is to reduce the slit pitch or increase the mask separation at a cost of FOV. Multiple RMCs or taking measurements with overlapping fields of view can also be employed to completely eliminate the blind zone. Once the source is located outside the blind zone the RMC transmission function becomes more distinct and ML-EM reconstruction generally provides a very accurate position estimate. Fig. 6 shows the RMC map for sources located in this region, and with the exception of the source measured at $\rho = 0$, all of the position estimates are very accurate. Table 2 summarizes some of the key statistics for this data generated using the bootstrap method discussed above.

The data in Table 2 demonstrate the RMCs ability to pinpoint the location of the source with a very high level of accuracy. As reported by Schnopper et al. [3] the uncertainty in the azimuthal angle is higher than the radial position, which can be understood by referencing the transmission function shown in Fig. 3. The radial position information is contained in the periodic peaks,

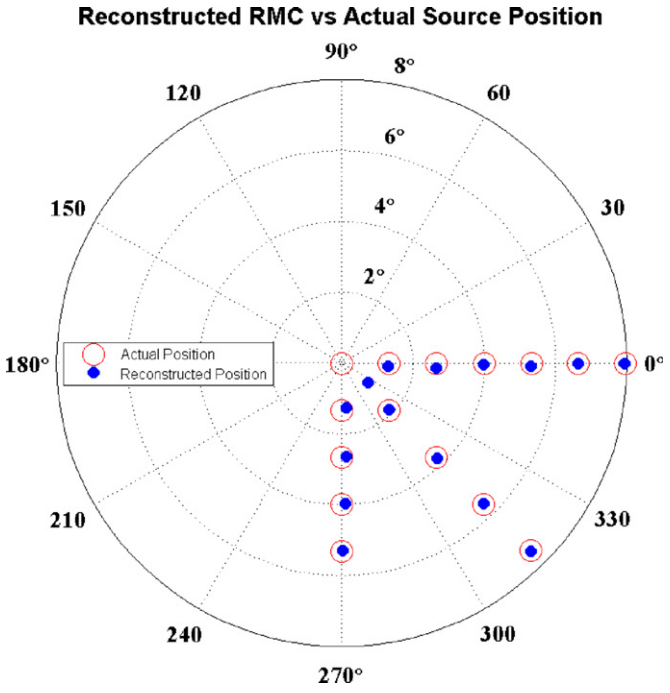

Fig. 6. Measurements with the prototype RMC in the active sensing region, show that position estimation using the ML-EM algorithm is very accurate. With the exception of the source located at $\rho = 0$, the average standard deviation on the position estimate for sources located between the blind zone and field of view edge is ~1.6 arc minutes.

Table 2
Statistics of interest for RMC position estimation in the active sensing region.

	Max error	Avg. error	Max std. dev. (1σ)	Avg. std. dev. (1σ)
ρ (arc min)	3	−0.24	2.01	1.12
ϕ (°)	6	0.16	4.56	2.44

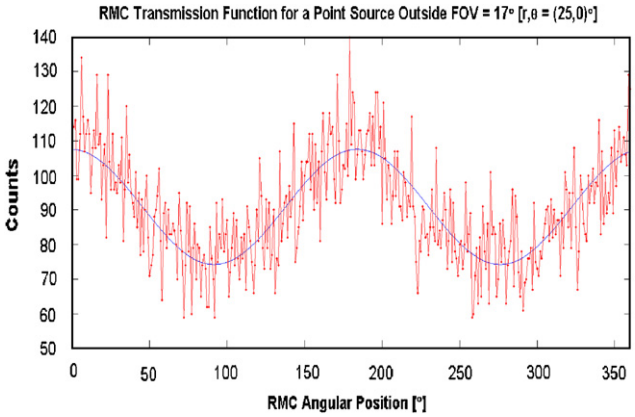

Fig. 7. A slight modulation occurs for sources outside the system FOV (Eq. (1)) that is caused by photons passing through the single mask closest to the detector. This figure shows data measured with the prototype RMC (FOV = ~17°) when the source is located at $\rho,\phi = (25,0)°$.

while the azimuthal position information is contained in the broad dip. When counting statistics and background are considered it is obvious that the broad dip will be less resolved than the peaks, leading to higher uncertainty in azimuth, ϕ.

The final region of interest is for sources located outside of the RMC FOV. Once the source moves beyond the two mask FOV, the projection of the front mask no longer overlaps the rear mask and detector. Photons still hit the rear mask however, and for masks with finite thickness they will be slightly modulated as the RMC rotates producing a transmission function like the one shown in Fig. 7.

One way to think of this is to consider the rear mask as a single two mask system with the mask separation parameter L, equal to the mask thickness t. An additional constraint is imposed because the top plane of the mask is physically connected to the lower plane. This means that photons entering a top slit must pass through the slit directly below it. This is in contrast to independent mask case, where the projection of the upper mask determines where the photon will hit the lower mask.

Through a simple inspection of geometry, it is possible to define the single mask FOV as

$$\mathrm{FOV}_{\mathrm{mask}} = \frac{s_{\max}}{t} \tag{4}$$

where $s_{\max}$ is the length of the longest mask slot and t is the mask thickness. For the designed system, the single mask FOV is ~79°. Also, as the source moves further off axis, the modulated component becomes increasingly small. Unfortunately the transmission functions in this region are too ill defined to produce a point location estimate using the ML-EM algorithm. It was found however, that when only a few iterations of the ML-EM algorithm are used, the general direction of the source in this region becomes known as shown in Fig. 8.

This general pointing information could presumably be used to position the RMC for a subsequent measurement. Once the source moves beyond the FOV of the two mask and single mask systems it will no longer be modulated, and simply becomes a dc background added to the total signal.

7. Conclusions

The performance of a rotating modulation imager was explored for point sources in near to mid-range fields. The current non-optimized system has a theoretical maximum position

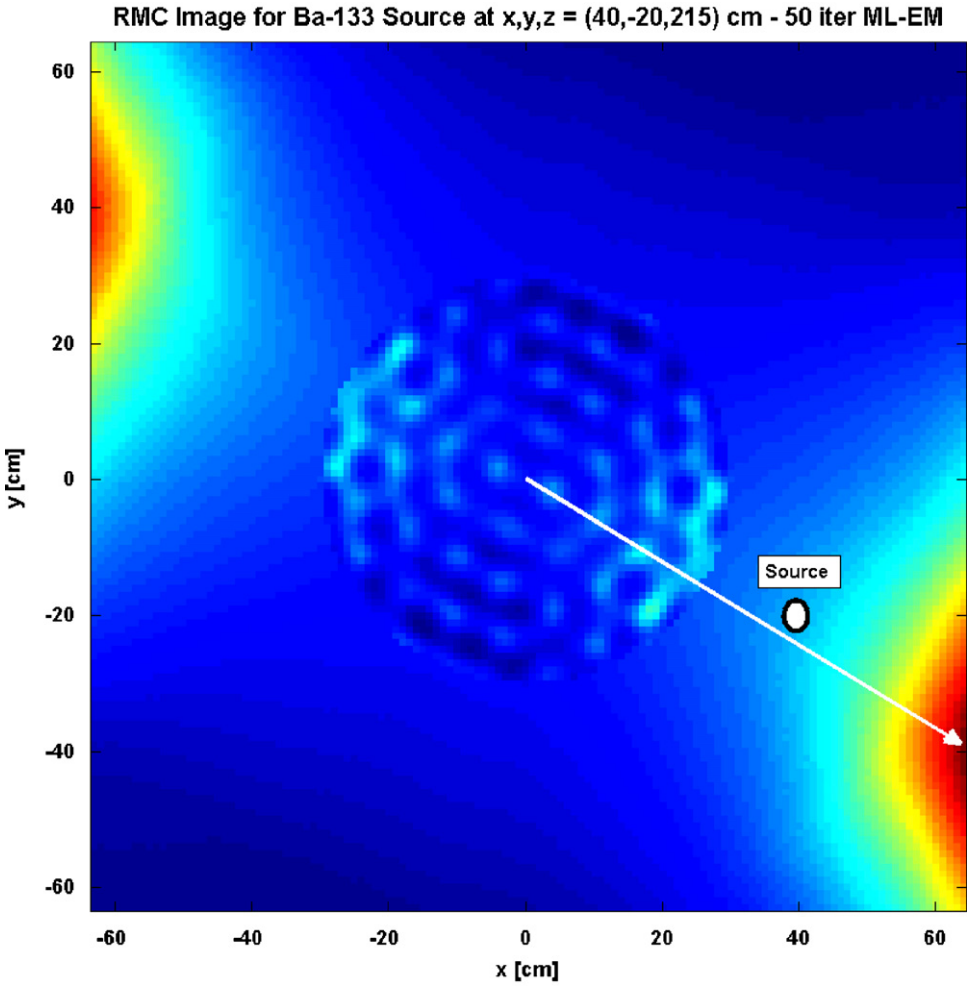

Fig. 8. Result from 50 iterations of ML-EM algorithm using measured data with the source at $x,y,z = (40,-20,215)$ cm. The point location estimate is not produced, but the broad edge region does point in the direction of the source indicated as a white circle.

resolution of $\sim 0.5^\circ$ with a $\sim 9^\circ$ field of view (FOV). When considering single detector RMC imaging, there are three regions that must be considered. The first region is a blind zone starting at the RMC axis of rotation and extending to a distance equal to the system resolution. Sources located in this region will be difficult if not impossible to locate. This zone can be minimized by decreasing the slit pitch or mask separation, which will increase the resolution. Multiple RMCs or measurements can also be employed to eliminate this blind zone.

The second region extends from the blind zone out to the two mask FOV given by Eq. (1). Sources in this region were located with an average deviation from the true source position (ρ,ϕ) of 1.14 arc minutes and 0.16°, respectively. The average standard deviations (1σ) for these location estimates was computed using a bootstrap method, where (ρ,ϕ) were 1.12 arc minutes and 2.24° respectively. As reported previously the error in the azimuthal direction is worse than the radial direction due to the difference in resolving the peaks (radial) in the transmission function versus the broad dip (azimuth) [3].

The final region extends from the two mask FOV out to a single mask FOV given by Eq. (3). Sources in this region are slightly modulated by the mask closest to the detector. At these locations the transmission functions are too ill-defined to generate a point location estimate using a ML-EM algorithm. The general direction of the source is produced when only a few iterations of the ML-EM algorithm are used. This information can then be used to help position the RMC for a subsequent measurement where the source may be in the system FOV.

It was also shown that the source ambiguity that is created with symmetric masks can be resolved for a single RMC by simply shifting one of the mask patterns slightly off axis so that it is no longer symmetric about the axis of rotation. This causes the transmission function to become asymmetric, which produces no ambiguities in the final reconstructed image. The cost for modifying the masks is a loss of modulation efficiency by $<1\%$ and a loss of geometric efficiency by 3.6%.

The performance of RMCs had been already demonstrated for both astronomical and medical imaging. From the data presented here, RMCs represent a practical way to locate point sources of interest to the homeland security community using any single non-position sensitive detector. Future research will focus on the relationship between the detector energy resolution and RMC angular resolution, the effects of mask penetrations on images and potential correction factors, the effects of multiple and extended source in the field of view, and adaptive imaging techniques for changing the RMC sampling profile during a measurement to locate sources faster.

References

[1] L. Mertz, in: Proceeding of the Symposium on Modern Optics, Polytechnic Press, New York, 1967, p. 787.

[2] A.P. Wilmore, Mon. Not. R. Astrom. Soc. 147 (1970) 387.
[3] Schnopper, et al., Space Sci. Rev. 8 (1968) 534.
[4] Akcasu, et al., Coded aperture gamma-ray imaging with stochastic apertures, Soc. Photo-Opt. Instr. Eng. Sem. App. Opt. Instr. Med., November 1973.
[5] S. Clinthorne, et al., IEEE Trans. Nucl. Sci. NS-1 (1995) 70–74.
[6] G.J. Hurford, et al., Solar Phys. 210 (1–2) (2002) 61–86.
[7] A.C. Sharma, et al, Design and development of a high-energy gamma camera for use with NSECT imaging: feasibility for breast imaging, in: IEEE TNS, vol. 54 (5), 2007, pp. 1498–1505.
[8] R.W. Johnson, An introduction to the bootstrap, Teaching Statistics, vol. 23 (2), Summer 2001, pp. 49–54.
[9] L.A. Shepp, Y. Vardi, IEEE Trans. Med. Imaging 1-1 (2) (1982) 113.